NUMERICAL SIMULATIONS FOR INVESTIGATION ON TRUE CAUSE OF THE TOTAL COLLAPSE OF THE WTC TOWERS

Daigoro ISOBE, *Dept. of Engineering Mechanics and Energy, University of Tsukuba*
        1-1-1 Tennodai, Tsukuba-shi, Ibaraki 305-8573, JAPAN
        Email: isobe@kz.tsukuba.ac.jp

Keywords: WTC towers, Collapse analysis, FEM, ASI-Gauss technique

SUMMARY

Although some official statements have been released by the Federal Emergency Management Agency (FEMA) and the National Institute of Standards and Technology (NIST), the 9/11 tragedy of the New York World Trade Center (WTC) towers still remains as an unresolved mystery since the towers collapsed totally to the ground, and, in an unnaturally rapid speed. We applied a low-cost, highly accurate collapse analysis code using the ASI-Gauss technique to several numerical simulations of framed structures, to seek the true cause of the highly-rapid total collapse. One of its applications is a full model simulation of the WTC 2 subjected under an aircraft impact. According to the simulation, "springback" phenomena due to rapid unloading were observed in the core columns during the impact, which might have caused the destruction of member joints. Another simulation carried out was that of the fire-induced collapse of a high-rise tower. The results clearly show the effect of the weak member joints, which were reported to be 20 to 30 % of the member strengths in the WTC towers, and also the effect of the strength reduction due to elevated temperatures. It is possible that the highly-rapid total collapse of the WTC towers was caused not only by the buckling and strength reduction of members due to elevated temperatures, but by the original weakness of the member joints and the destruction of those during the collision of the aircraft.

1. INTRODUCTION

The 9/11 terrorist attack on the New York World Trade Center (WTC) towers caused an unprecedented tragedy in the history of architecture. The twin towers WTC 1 and 2 stood in flames caused by jet fuel until finally, both collapsed totally to the ground with thousands of people trapped in the buildings. Both towers collapsed at an unnaturally high speed, which was observed to be nearly equal to that of free fall. Official statements have already been released by the Federal Emergency Management Agency (FEMA) in 2002 [ASCE/FEMA, 2002], and also by the National Institute of Standards and Technology (NIST) in 2005 [NIST NCSTAR1, 2005], regarding the incident. FEMA concluded in the report that the heat of burning jet fuel induced additional stresses into the damaged structural frames while simultaneously softening and weakening these frames, and this additional loading and the resulting damage were sufficient to induce the collapse of both structures. Many detailed numerical analyses were carried out in [NIST NCSTAR1, 2005], and the report was concluded by stating "the WTC towers likely would not have collapsed under the combined effects of aircraft impact damage and the extensive, multifloor fires, if the thermal insulation had not been widely

dislodged or had been only minimally dislodged by aircraft impact." But, did the fire really spread to such a wide range in the buildings to cause the total collapse? Moreover, was the heat high enough to reduce the strengths of structural members? What really caused the free-fall total collapse? Many questions still remain unresolved. Also, it is to be noted that although many detailed analyses were performed in [NIST NCSTAR1, 2005], not even a single result can be found showing the dynamic behaviors of the towers during aircraft impact. It is clear that the towers experienced an extreme dynamic load that no other high-rise building has ever experienced in history. Therefore, we first performed an aircraft impact analysis of a full-model WTC tower, to determine the possibility of the impact itself acting as a fatal cause of the collapse. We then carried out some fire-induced collapse analyses of a high-rise tower to verify the influence of fire patterns, member strengths and member joint strengths against collapse phenomena. The collapse phase is a very dynamic phenomenon, but the phase before collapse initiation is a very static one and the calculation cost may increase to analyze the whole process. Therefore, the numerical code must be a highly accurate, less-memory-consuming one, and has to be reliable
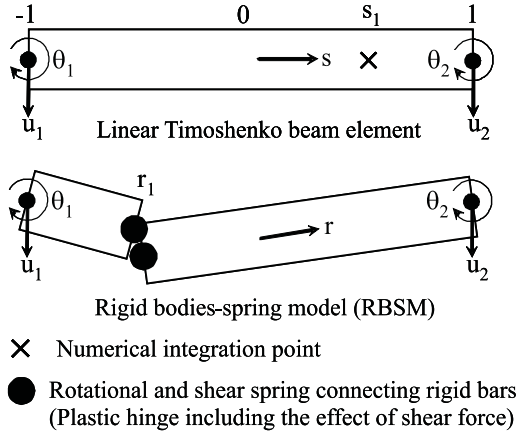
Linear Timoshenko beam element

Rigid bodies-spring model (RBSM)

×   Numerical integration point

●   Rotational and shear spring connecting rigid bars
(Plastic hinge including the effect of shear force)

Figure 1 Linear Timoshenko beam element and its physical equivalent

×   Numerical integration point $s_g = 1 - (2/\sqrt{3})$

●   Stress evaluation point $r_g = -1 + (2/\sqrt{3})$

Figure 2 Locations of numerical integration and stress evaluation points in ASI-Gauss technique

when member fracture and contact are taken into account.

The numerical code used in the analyses is based on the ASI-Gauss technique [Lynn and Isobe, 2007], which was modified from the adaptively shifted integration (ASI) technique [Toi and Isobe, 1993] for the linear Timoshenko beam element. It enables the computation of highly accurate elastoplastic solutions even with the minimum number of elements per member. In this paper, we first describe an outline of the technique and the modeling of the WTC tower, followed by an aircraft impact simulation result on WTC 2, and some fire-induced collapse simulation results on a high-rise tower.

2. ASI-GAUSS TECHNIQUE

Figure 1 shows a linear Timoshenko beam element and its physical equivalence to the RBSM. As shown in the figure, the relationship between the locations of the numerical integration point and the stress evaluation point where a plastic hinge is formed is expressed [Toi, 1991] as

$$r = -s \tag{1}$$

In the above equation, s is the location of the numerical integration point and r is the location where stresses and strains are evaluated. s and r are nondimensional quantities that take values between -1 and 1.

In both the ASI and ASI-Gauss techniques, the numerical integration point is shifted adaptively when a fully plastic section is formed within an element to form a plastic hinge exactly at that section. When the plastic hinge is unloaded, the corresponding numerical integration point is shifted back to its normal position. Here, the normal position means the location where the numerical integration point is placed when the element acts elastically. By doing so, the plastic behavior of the element is simulated
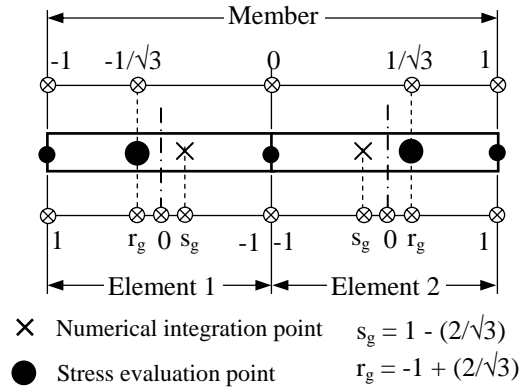
appropriately, and the converged solution is achieved with only a small number of elements per member. However, in the ASI technique, the numerical integration point is placed at the midpoint of the linear Timoshenko beam element, which is considered to be optimal for one-point integration, when the entire region of the element behaves elastically. When the number of elements per member is very small, solutions in the elastic range are not accurate since one-point integration is used to evaluate the low-order displacement function of the beam element.

The main difference between the ASI and ASI-Gauss techniques lies in the normal position of the numerical integration point. In the ASI-Gauss technique, two consecutive elements forming a member are considered as a subset, as shown in Fig. 2, and the numerical integration points of an elastically deformed member are placed such that the stress evaluation points coincide with the Gaussian integration points of the member. This means that stresses and strains are evaluated at the Gaussian integration points of elastically deformed members. Gaussian integration points are optimal for two-point integration and the accuracy of bending deformation is mathematically guaranteed [Press et al, 1992]. In this way, the ASI-Gauss technique takes advantage of two-point integration while using one-point integration in actual calculations.

Structurally discontinuous problems also become easily handled using the ASI and ASI-Gauss techniques by shifting the numerical integration point of the linear Timoshenko beam element to an appropriate position and by releasing the resultant forces in the element simultaneously. Material strains are used for the fracture criterion. Elemental contact is considered in the code by introducing gap elements between pairs of elements determined to be in contact by geometrical relations. More details on the code can be found in [Lynn and Isobe, 2007] and [Isobe and Sasaki, 2007].
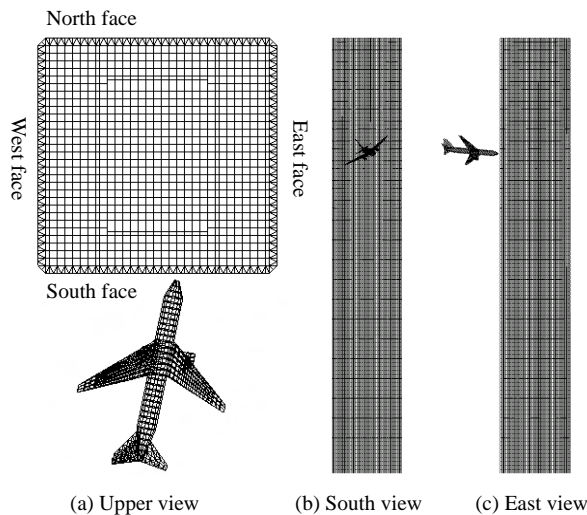
North face

West face

East face

South face

(a) Upper view   (b) South view   (c) East view

Figure 3 Analyzed model

Core beam

Core column

Main
double truss

Spandrel

Transverse truss

Perimeter
column   Diagonal
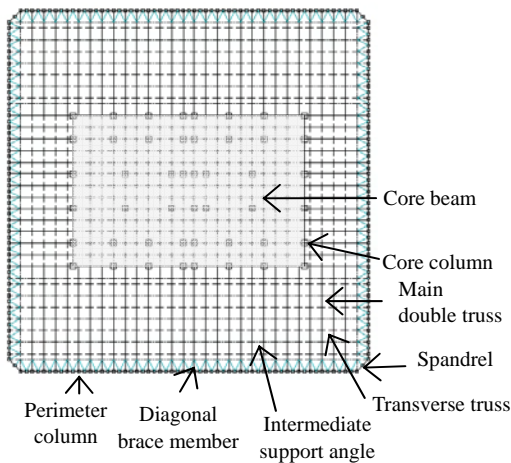brace member   Intermediate
support angle

Figure 4 Cross section of the WTC towers

3. NUMERICAL INVESTIGATIONS

Several numerical simulations are performed on a full-model WTC tower and a high-rise tower, to seek the true cause of the highly-rapid collapse of the WTC towers.

3.1 Aircraft Impact Analysis of the World Trade Center Tower

We performed an analysis of the aircraft impact with a full-scale model of WTC Tower 2 [Isobe and Sasaki, 2007] using the code described in the previous section. Details on the structural members and construction data are extracted and adopted from previous reports ([ASCE/FEMA, 2002] and [NIST NCSTAR1, 2005]). The tower and the B767-200ER aircraft are both modeled using linear Timoshenko beam elements, of which all members are subdivided into two elements. Figure 3 shows a schematic view of the WTC 2 tower model and the aircraft model. The tower model contains 604,780 elements, 435,117 nodes and 2,608,686 degrees of freedom, while the aircraft model contains 4,322 elements, 2,970 nodes and 17,820 degrees of freedom. Figure 4 shows a

cross-sectional view of the towers. A floor is roughly divided into two sections, external and core structures, each with different roles from the structural point of view. The external structure is mainly designed to sustain wind loads, while the main double trusses connected to the core structure support the floor loads. The whole tower is subjected to a designed dead load of 2,890 MN and 40 % of the allowed capacity load, 300 MN. The ratio of the loads between the core and external structures is adjusted to become approximately 6:4 [ASCE/FEMA, 2002]. All structural members of the B767-200ER aircraft are assumed to have box-shaped cross sections and the material properties of extra super duralumin. The total mass of the aircraft at the time of impact is 142.5 t, which is the sum of the masses of the aircraft (112.5 t) and the jet fuel (30 t). The mass of each
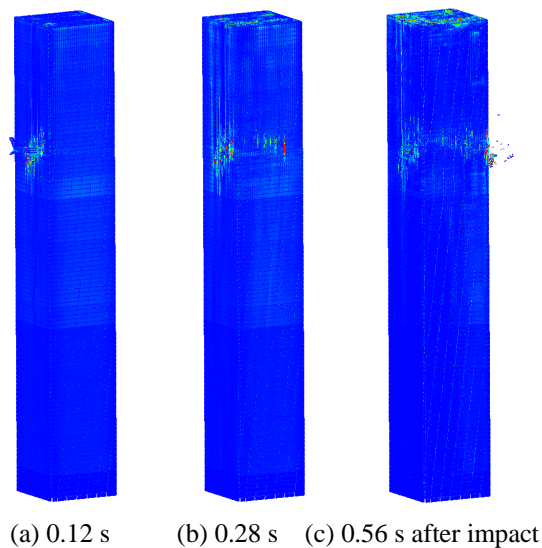

(a) 0.12 s   (b) 0.28 s   (c) 0.56 s after impact

Figure 5 Moment of impact (global view)

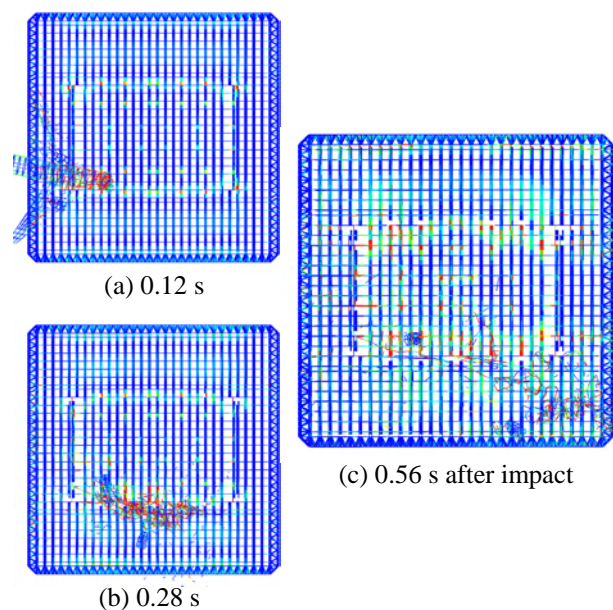
(a) 0.12 s

(c) 0.56 s after impact

(b) 0.28 s

Figure 6 Motion of fuselage and engines (upper view)

Table 1 Impact timeline of the B767-200ER aircraft

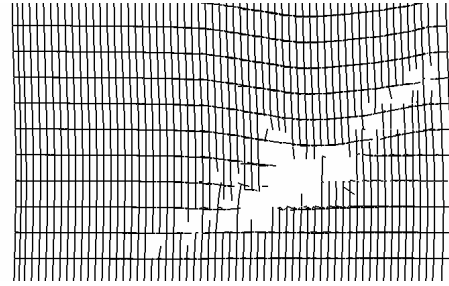| Phase	Elapsed time (s)	B767-200ER aircraft		
		Left engine	Right engine	Snout
	0.0	Snout hits outer-perimeter wall		
A	0.048			Hits core structure
	0.072	Hits outer-perimeter wall		
B	0.076		Hits outer-perimeter wall	
C	0.128	Hits core structure		
D	0.168	Hits core column No.902		
E	0.504	Hits core column No.903		
F	0.512		Hits east side outer-perimeter wall	
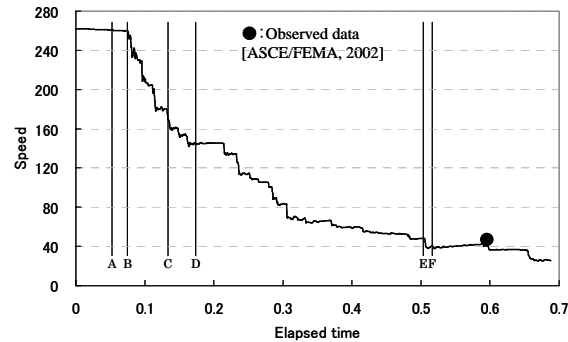
Figure 7 Velocity curve of the right engine

engine is assumed to be 19.315 t. The nose of the aircraft is tilted 11.5 degrees to the east and 5 degrees downward, and its left wing is inclined downward by 35 degrees. It is assumed to collide with the 81st floor on the south face of WTC 2 with a cruising speed of 590 mph (262 m/s).

Most of the column joints were connected with 34-mm-thick end plates attached by 4 to 6 bolts. The joints were weak against flexural and shear forces; the simple moment capacity of the bolt group was 20 to 30 % of the plastic moment capacity of the column itself [ASCE/FEMA, 2002]. The beam joints of main double trusses also had simple connections to sustain static, vertical dead loads, which satisfied the initial structural design. The structural design of member joints in Japan, for example, demands the capacity to be greater than that of the member itself. In the present analysis, the vulnerability of member joints are considered by introducing fracture conditions as follows [Lynn and Isobe, 2007]:

$$\left|\frac{\kappa_x}{\kappa_{fx}}\right| - 1 \geq 0 \;\; or \;\; \left|\frac{\kappa_y}{\kappa_{fy}}\right| - 1 \geq 0 \;\; or \;\; \left(\frac{\epsilon_z}{\epsilon_{fz}}\right) - 1 \geq 0 \quad (2)$$

where κ_x, κ_y, ϵ_z, κ_{fx}, κ_{fy} and ϵ_{fz} are the bending strains

(a) Numerical result
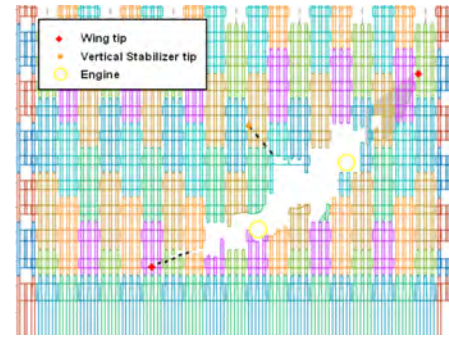
(b) Observed data [NIST NCSTAR1, 2005]

Figure 8 Damage of the WTC 2 south face

around the x- and y-axes, the axial tensile strain and the critical values for these three strains, respectively. In the present analysis, we fixed the critical strain values by comparing the impact damage and motion of the engines with the observed data. We also considered the strain rate effect on yield strength using the Cowper-Symonds equation [Jones, 1989]. An implicit scheme with a consistent mass matrix is adopted. No damping except for the algorithmic one is applied. δ is set to 5/6 and β to 4/9 in Newmark's β method [Press et al, 1992]. The time increment Δt is set to 0.2 ms. An updated Lagrangian formulation is used since large deformations are expected in the analysis, and the conjugate gradient (CG) method is used as the solver to reduce the memory requirement. The analytical code is run on a high-performance computer (1.4 GHz Itanium*2, 8GB RAM), and the calculation takes approximately two months for a physical time of 0.7 s.

The numerical results are shown in Figs. 5 and 6. Fractured elements are deleted in the figures. It is observed that the left engine reduces its speed rapidly as it directly enters the core structure. The right engine, on the other hand, glances off the core structure and passes through the north-east corner of the tower. Table 1 shows the impact timeline of the fuselage and both engines. The velocity curve of the right engine is shown in Fig. 7 and a comparison of the damaged surfaces between the numerical result and the observed data [NIST NCSTAR1, 2005] is shown in Fig. 8. Both results are in good agreement with the observed data. Figure 9 shows the transition of axial forces in typical core columns every ten
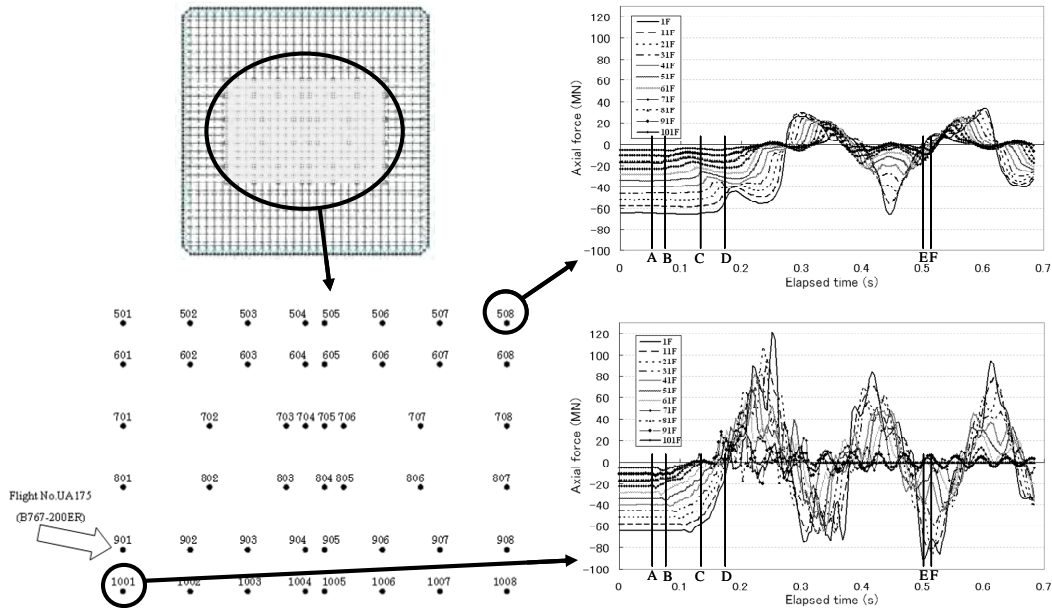
Figure 9 Time histories of axial forces in core columns No.508 and No.1001
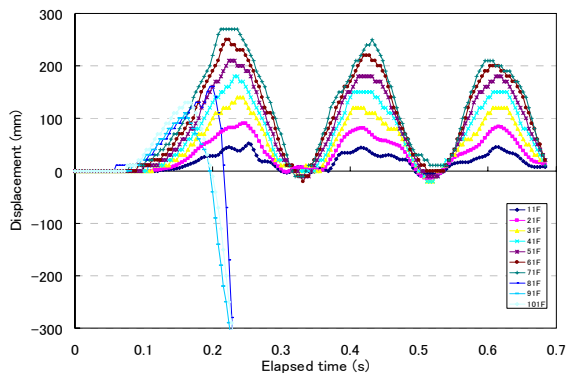

Figure 10 Axial displacement due to spring-back phenomena (core column No. 1001)
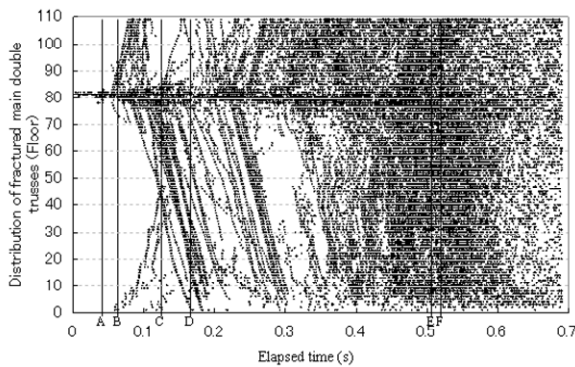

Figure 11 Distribution of fractured main double trusses

stories from the ground floor to the top floor. The core columns are compressed constantly until the snout of the aircraft reaches the core structure (Phase A in the figure), after which a wave due to the impact and member fracture propagates in the horizontal and vertical directions. In particular, the compression decreases instantaneously in the fractured core column (No. 1001) at the floors above the impact point. At the lower levels, compression changes to tension immediately after the left engine hits the core structure (Phase C), and the values of axial forces continue to vibrate with large amplitude. Note that the lower the height, the larger the amplitude becomes. The core column No.1001 at the 60th floor, for example, moves vertically for 25 cm in 0.2 s as a result of this dynamic transition (see Fig. 10).

What actually caused this dynamic unloading large enough to generate such large tensile forces? We extracted the time history of the distribution of fractured main double trusses, as shown in Fig. 11, to investigate the cause. The propagation of fractured trusses from the impact point to upper and lower levels can be observed in the figure. This propagation speed almost matched the longitudinal wave speed in the columns. It can be assumed that the shock wave due to impact propagated through the tower and occasionally reflected to other columns at the ground or top levels, destroying each member joint as it moved on.

Our assumed scenario is as follows; the aircraft impact destroyed several main double trusses, that supported the floor slabs, and led to a middle-class unloading of core columns. The deformation due to the unloading caused other trusses to disconnect, which released further burden from the core columns. This disconnect-and-release process advanced rapidly in a chain reaction manner and a spring-back phenomenon might have occurred in many columns in such a way that a compressed spring is released in a very short moment. It was fatal enough to produce a gigantic tensile force on the columns, which might have triggered the total fracture of some column joints, eventually leading to the total collapse of the
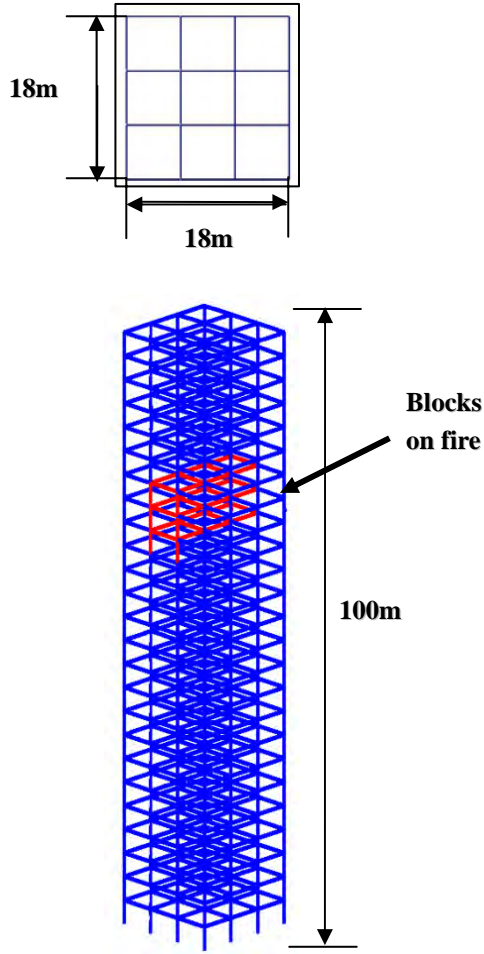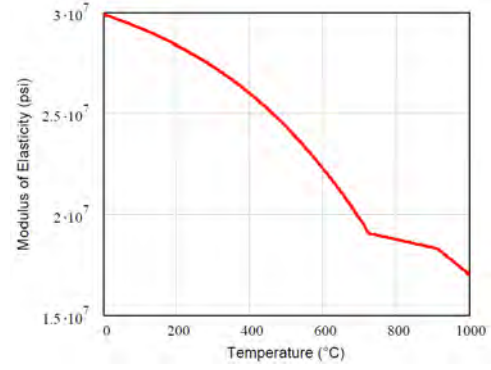
Figure 12 High-rise tower model

(a) Elastic modulus

— Construction Steel
····· Bolt Steel

(b) Yield strength

Figure 13 Strength reduction curves of steel due to elevated temperatures

towers. It can be assumed that the damage in lower levels was larger, since the lower the level went, the larger the tensile force became.
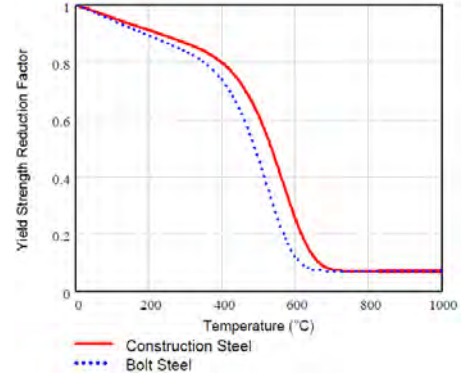
3.2 Fire-Induced Collapse Analyses of High-Rise Towers

Some analyses of fire-induced collapse are carried out on a 25-story 3-span tower as shown in Fig. 12 to determine the effect of the strength reduction due to elevated temperatures. We used a model with two cases of column thickness; thick type ($\square$-600×600 ×18×18 at the 1st floor) and thin type ($\square$-430×430 ×13×13 at the 1st floor), two cases of member joint strengths; strong type (C_M=1.0) and weak type (C_M=0.2), and three cases of fire patterns; 17th ~ 19th floors with 3 blocks (symmetry), 4 blocks (asymmetry) and 9 blocks (all floor) on fire. The joint strength ratio C_M indicates the ratio of member joint strength against the member strength itself. The value is directly used in the yield function as follows, to explicitly express the influence of member joint strength:

$$f = \left(\frac{M_x}{C_M M_{x0}}\right)^2 + \left(\frac{M_y}{C_M M_{y0}}\right)^2 + \left(\frac{N}{N_0}\right)^2 + \left(\frac{M_z}{M_{z0}}\right)^2 - 1 = 0 \quad (3)$$

The ratio value is assumed on the basis of the fact that the member joint strengths of typical core columns were about 20 to 30 % of those of the members in the WTC towers [ASCE/FEMA, 2002]. Here, the fracture condition of member joints are considered by examining bending strains, axial tensile strain and shear strains in a member, as follows:

$$\left|\frac{\kappa_x}{\kappa_{fx}}\right| - 1 \geq 0 \quad \text{or} \quad \left|\frac{\kappa_y}{\kappa_{fy}}\right| - 1 \geq 0 \quad \text{or} \quad \left(\frac{\epsilon_z}{\epsilon_{fz}}\right) - 1 \geq 0$$

$$\text{or} \quad \left|\frac{\gamma_{xz}}{\gamma_{fxz}}\right| - 1 \geq 0 \quad \text{or} \quad \left|\frac{\gamma_{yz}}{\gamma_{fyz}}\right| - 1 \geq 0 \quad (4)$$

where γ_{xz}, γ_{yz}, γ_{fxz}, γ_{fyz} are the shear strains for the x- and y-axes and the critical values for the strains, respectively. The critical strain values used here are the values actually obtained from some experiments concerning the high strength joint bolts [Hirashima et al, 2007]. Curves showing the reduced elastic modulus and yield strength of steel due to elevated temperatures [NIST NCSTAR1, 2005], as shown in Figs. 13(a) and 13(b), are adopted. The elastic modulus of the columns with no thermal insulation is reduced to 60 % of the original value, and the yield strength to 10 % of the original strength, at 700 ℃, which is a natural temperature in normal fire. We assumed the temperature to rise up to 700 ℃ in 7
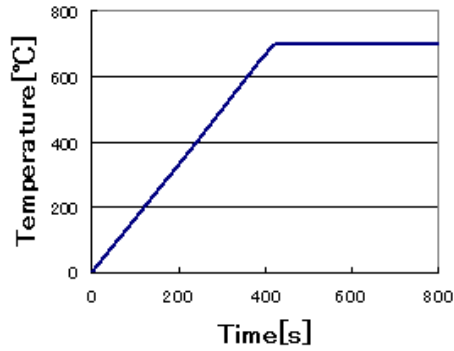
Figure 14 Assumed time history of temperature

minutes as shown in Fig. 14. Also, we applied a time increment control to enable continuous calculation from static to dynamic phenomena.

Two of the numerical results are shown in Figs. 15 and 16. Both are performed with the thin-column type model. Figure 15 shows the result with 3-floors 4-blocks on fire and Fig. 16 with 3-floors 9-blocks on fire, each performed on strong-member-joint type (C_M=1.0) and weak-member-joint type (C_M=0.2). We can clearly see the difference in collapse modes between the two models in both figures. The strong-member-joint models initiate to collapse once they buckle at the floors that are on fire, but withstand to collapse any further by redistributing the stresses in the towers. The weak-member-joint models, on the other hand, fail to stop the progression of collapse and end in a total destruction. Table 2 shows the sum of all the results. It can be concluded that the possibility of total collapse becomes high, in spite of thickness of the columns, when the joint strength ratio is low. Fire patterns do have influence on the possibility of collapse. Multi-floor and asymmetric fire patterns may increase the possibility of collapse. And furthermore, the collapse speeds were much slower than the free-fall or saturated speed in these cases, which does not explain the high-speed collapse of the WTC towers.

4. CONCLUSION

The numerical results shown in this paper might indicate that the highly-rapid total collapse of the
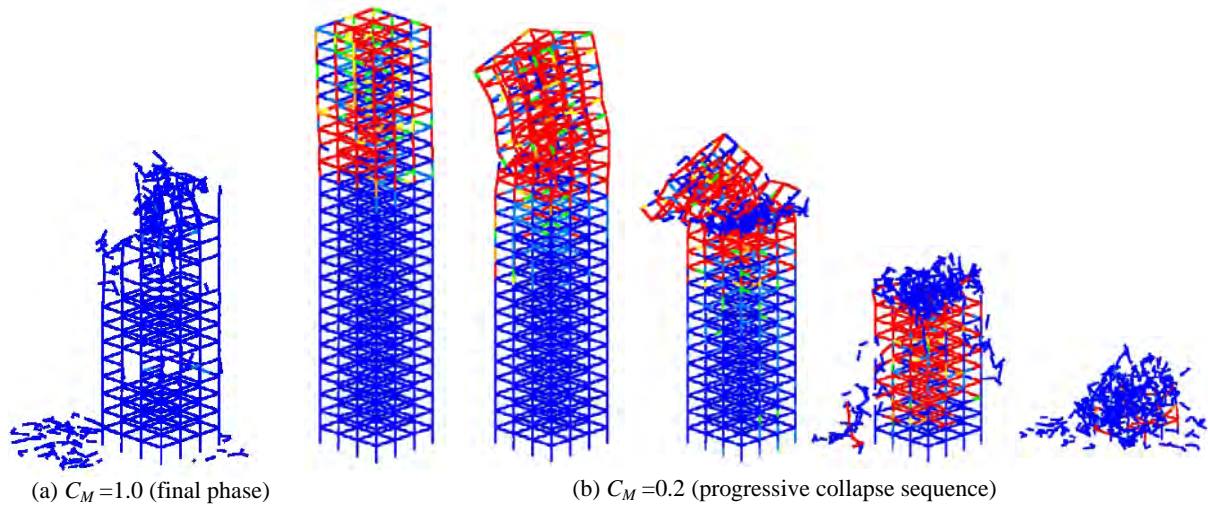

(a) C_M =1.0 (final phase)　　　　　　　　　　　(b) C_M =0.2 (progressive collapse sequence)

Figure 15 Fire-induced collapse analysis with 3F-4 blocks fire pattern (thin column model)

(a) C_M =1.0 (final phase)　　　　　　　　　　　(b) C_M =0.2 (progressive collapse sequence)
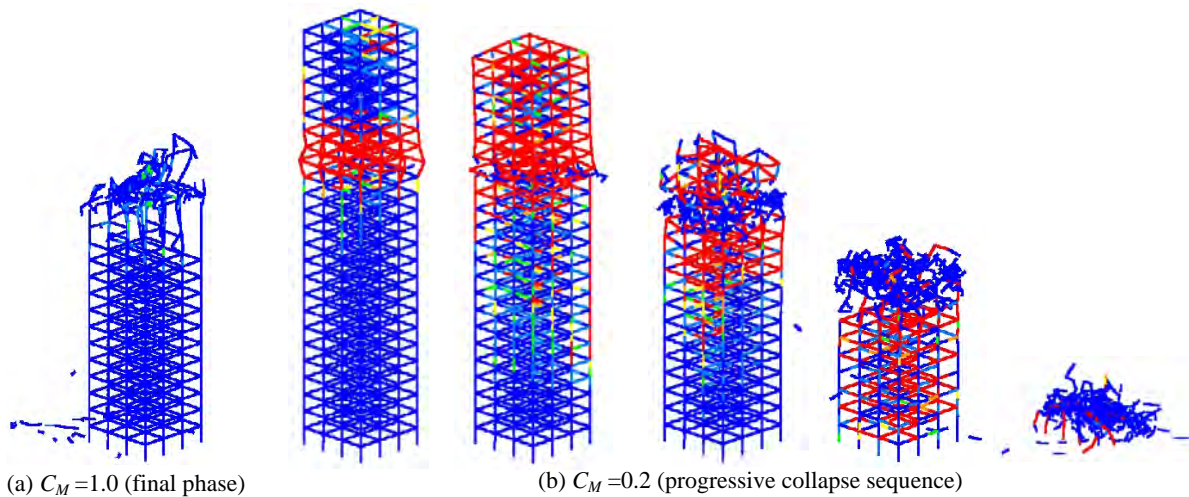
Figure 16 Fire-induced collapse analysis with 3F-9 blocks fire pattern (thin column model)

Table 2 Collapse modes occurred in the fire-induced collapse analyses

Columns	Joint strength ratio C_M	3F 3 blk. fire	3F 4 blk. fire	3F 9 blk. fire
□-600×600× 18×18 → □-400×400× 12×12	1.0	No collapse	Total collapse (496s)	Partial collapse (421s)
	0.2	Total collapse (886s)	Total collapse (463s)	Total collapse (423s)
□-430×430× 13×13 → □-230×230×7 ×7	1.0	No collapse	Partial collapse (433s)	Partial collapse (417s)
	0.2	Total collapse (516s)	Total collapse (420s)	Total collapse (412s)

( ): Collapse initiation time

WTC towers was caused not only by the buckling and strength reduction of members due to elevated temperatures, but by the original weakness of the member joints and the destruction of those during the collision of the aircraft. Further investigations by performing full-model fire-induced collapse analyses of the WTC towers are scheduled.

5. REFERENCES

ASCE/FEMA (2002), *World Trade Center Building Performance Study: Data Collection, Preliminary Observation and Recommendations*.

Hirashima, T., Hamada, N., Ozaki, F., Ave, T. and Uesugi, H. (2007), "Experimental Study on Shear Deformation Behavior of High Strength Bolts at Elevated Temperature", *J. Struct. Constr. Eng., AIJ*, No.621, pp. 175-180, in Japanese.

Isobe, D. and Sasaki, Z. (2007), "Aircraft Impact Analyses of the World Trade Center Towers", *CD-ROM Proc. of 1st Int. Workshop on Performance, Protection, and Strengthening of Structures under Extreme Loading (PROTECT2007)*, Whistler, Canada.

Jones, N. (1989), *Structural impact*, New York: Cambridge University Press.

Lynn, K.M. and Isobe, D. (2007), "Finite Element Code for Impact Collapse Problems of Framed Structures", *Int. J. Numer. Meth. Eng.,* Vol. 69, No. 12, pp. 2538-2563.

NIST NCSTAR 1 (2005), *Federal Building and Fire Safety Investigation of the World Trade Center Disaster: Final Report on the Collapse of the World Trade Center Towers*, National Institute of Standards and Technology (NIST).

Press, W.H., Teukolsky, S.A., Vetterling, W.T. and Flannery, B.P. (1992), *Numerical Recipes in FORTRAN: The Art of Scientific Computing*, New York: Cambridge University Press.

Toi, Y. (1991), "Shifted Integration Technique in One-Dimensional Plastic Collapse Analysis Using Linear and Cubic Finite Elements", *Int. J. Numer. Meth. Eng.*, Vol. 31, pp. 1537-1552.

Toi, Y. and Isobe, D. (1993), "Adaptively Shifted Integration Technique for Finite Element Collapse Analysis of Framed Structures", *Int. J. Numer. Meth. Eng.*, Vol. 36, pp. 2323-2339.